

# Time Empirical Ionospheric Correction Model (STORM) response in IRI2000 and challenges for empirical modeling in the future

E. A. Araujo-Pradere and T. J. Fuller-Rowell

Cooperative Institute for Research in Environmental Sciences, University of Colorado and Space Environment Center,  
National Oceanic and Atmospheric Administration, Boulder, Colorado, USA

D. Bilitza

Raytheon Information Technology and Scientific Services, Goddard Space Flight Center, Greenbelt, Maryland, USA

Received 24 October 2002; revised 2 April 2003; accepted 25 April 2003; published 16 January 2004.

[1] IRI2000 [Bilitza, 2001] now contains a geomagnetic activity dependence based on the Time Empirical Ionospheric Correction Model (STORM) [Araujo-Pradere and Fuller-Rowell, 2002; Araujo-Pradere *et al.*, 2002]. The storm correction is driven by the previous time history of  $a_p$  and is designed to scale the quiet time  $F$  layer critical frequency ( $f_oF_2$ ) to account for storm-time changes in the ionosphere. The quality of the storm-time correction was recently evaluated by comparing the model with the observed ionospheric response during all the significant geomagnetic storms in 2000 and 2001. The model output was compared with the actual ionospheric response at 15 stations for each storm. These quantitative comparisons using statistical metrics showed that the model captures the decreases in electron density particularly well in summer and equinox conditions, but is not so good during winter conditions. To further assess the capabilities of the model, STORM has been compared in detail with observations during the Bastille Day storm in July 2000. This storm, considered to be on the extreme end of the statistical scale of storm magnitude, highlights two main areas where challenges remain for the empirical storm-time ionospheric model. The first is the rapid onset of the positive storm phase; the second is the regional composition changes that can affect one longitude sector at the expense of another for a particular storm. Both these challenges, although appreciated during the development of STORM, remain to be addressed.

**INDEX TERMS:** 2447 Ionosphere: Modeling and forecasting; 2435 Ionosphere: Ionospheric disturbances; 2427 Ionosphere: Ionosphere/atmosphere interactions (0335);

**KEYWORDS:** ionospheric modeling, empirical modeling, geomagnetic storms, ionospheric storms, validation

**Citation:** Araujo-Pradere, E. A., T. J. Fuller-Rowell, and D. Bilitza (2004), Time Empirical Ionospheric Correction Model (STORM) response in IRI2000 and challenges for empirical modeling in the future, *Radio Sci.*, 39, RS1S24, doi:10.1029/2002RS002805.

## 1. Introduction

[2] The International Reference Ionosphere (IRI) is an international project sponsored by the Committee on Space Research (COSPAR) and the International Union of Radio Science (URSI). These organizations formed a Working Group in the late 1960s to produce an empirical standard model of the ionosphere, based on all available data sources. Several steadily improved editions of the model have been released. For a given location, time, and

date, IRI describes the electron density, electron temperature, ion temperature, and ion composition in the altitude range from about 50 to about 2000 km; and also the electron content. It provides monthly averages for magnetically quiet conditions. The major data sources are the worldwide network of ionosondes, the powerful incoherent scatter radars, the ISIS and Alouette topside sounders, and in situ instruments on several satellites and rockets [Bilitza *et al.*, 1993]. One missing feature was that, before the release of IRI2000 [Bilitza, 2001], the IRI model had no geomagnetic activity dependence.

[3] The understanding of the ionospheric response to magnetic perturbations has reached a level where part of

**Table 1.** Average RMSE for All the Storms in the 2000–2001 Period<sup>a</sup>

Storms	Models	North Hemisphere								South Hemisphere							
		Days					Averages			Days					Averages		
		1	2	3	4	5	Storm	Day	% Imp	1	2	3	4	5	Storm	Day	% Imp
7 Apr 2000	IRI95	1.22	1.26	<b>2.88</b>	1.30	0.91	1.51	<b>2.88</b>	<b>49</b>	1.94	1.82	<b>3.03</b>	1.59	1.70	2.02	<b>3.03</b>	<b>31</b>
	IRI2000	1.19	1.18	<b>1.45</b>	1.33	0.91	1.21	<b>1.45</b>		1.94	1.88	<b>2.10</b>	1.72	1.70	1.87	<b>2.10</b>	
24 May 2000	IRI95	0.86	<b>2.25</b>	<b>1.37</b>	0.95	0.79	1.24	<b>1.81</b>	<b>51</b>	2.00	<b>1.56</b>	<b>1.38</b>	1.18	1.13	1.45	<b>1.47</b>	<b>−3</b>
	IRI2000	0.89	<b>1.01</b>	<b>0.76</b>	0.87	0.79	0.86	<b>0.88</b>		2.01	<b>1.60</b>	<b>1.44</b>	1.20	1.14	1.48	<b>1.52</b>	
15 Jul 2000	IRI95	1.03	0.96	<b>1.70</b>	<b>2.75</b>	1.08	1.51	<b>2.23</b>	<b>49</b>	1.17	1.07	<b>1.19</b>	<b>1.33</b>	1.27	1.20	<b>1.26</b>	<b>−6</b>
	IRI2000	0.90	0.85	<b>1.05</b>	<b>1.21</b>	0.82	0.97	<b>1.13</b>		1.20	1.19	<b>1.16</b>	<b>1.51</b>	1.27	1.26	<b>1.33</b>	
12 Aug 2000	IRI95	1.24	<b>1.94</b>	<b>2.94</b>	<b>1.99</b>	1.14	1.85	<b>2.29</b>	<b>40</b>	1.16	<b>1.28</b>	<b>1.56</b>	<b>1.17</b>	1.10	1.25	<b>1.34</b>	<b>−5</b>
	IRI2000	1.17	<b>1.47</b>	<b>1.50</b>	<b>1.18</b>	1.13	1.29	<b>1.38</b>		1.15	<b>1.28</b>	<b>1.55</b>	<b>1.36</b>	1.08	1.28	<b>1.40</b>	
17 Sep 2000	IRI95	1.43	1.50	<b>2.05</b>	<b>3.36</b>	2.28	2.12	<b>2.70</b>	<b>38</b>	2.01	1.80	<b>2.57</b>	<b>3.59</b>	2.06	2.41	<b>3.08</b>	<b>22</b>
	IRI2000	1.37	1.31	<b>1.63</b>	<b>1.74</b>	1.54	1.52	<b>1.69</b>		1.74	1.67	<b>2.24</b>	<b>2.58</b>	1.74	2.00	<b>2.41</b>	
5 Oct 2000	IRI95	1.80	<b>1.74</b>	<b>2.75</b>	<b>1.64</b>	0.92	1.77	<b>2.04</b>	<b>32</b>	0.78	<b>1.62</b>	<b>3.68</b>	<b>1.55</b>	1.00	1.72	<b>2.28</b>	<b>32</b>
	IRI2000	1.63	<b>1.46</b>	<b>1.63</b>	<b>1.06</b>	0.87	1.33	<b>1.38</b>		0.72	<b>1.33</b>	<b>2.26</b>	<b>1.09</b>	0.99	1.28	<b>1.56</b>	
20 March 2001	IRI95	1.14	<b>2.83</b>	1.53	0.97	1.46	1.58	<b>2.83</b>	<b>37</b>	1.83	<b>4.23</b>	2.46	1.06	1.18	2.15	<b>4.23</b>	<b>19</b>
	IRI2000	1.06	<b>1.80</b>	1.38	0.88	1.23	1.27	<b>1.80</b>		1.90	<b>3.44</b>	1.85	1.01	1.05	1.85	<b>3.44</b>	
31 March 2001	IRI95	0.88	<b>3.28</b>	<b>2.04</b>	1.30	1.26	1.75	<b>2.66</b>	<b>34</b>	2.01	<b>3.10</b>	<b>3.79</b>	1.49	1.34	2.35	<b>3.45</b>	<b>−3</b>
	IRI2000	0.98	<b>1.85</b>	<b>1.67</b>	1.22	1.37	1.42	<b>1.76</b>		2.17	<b>3.55</b>	<b>3.52</b>	1.61	1.47	2.47	<b>3.54</b>	
11 April 2001	IRI95	1.63	1.49	<b>2.63</b>	1.62	1.88	1.85	<b>2.63</b>	<b>48</b>	1.21	1.66	<b>3.94</b>	1.56	2.99	2.27	<b>3.94</b>	<b>31</b>
	IRI2000	1.54	1.31	<b>1.36</b>	1.35	1.59	1.43	<b>1.36</b>		1.21	1.55	<b>2.72</b>	1.46	2.51	1.89	<b>2.72</b>	
18 April 2001	IRI95	0.98	<b>2.43</b>	1.60	0.86	0.59	1.29	<b>2.43</b>	<b>31</b>	1.21	<b>2.10</b>	1.82	1.45	1.28	1.57	<b>2.10</b>	<b>6</b>
	IRI2000	0.87	<b>1.66</b>	1.36	0.79	0.58	1.05	<b>1.66</b>		1.24	<b>1.97</b>	1.85	1.42	1.25	1.54	<b>1.97</b>	
25 Sept. 2001	IRI95	1.78	0.98	<b>1.70</b>	1.38	1.37	1.44	<b>1.70</b>	<b>31</b>	1.70	1.08	<b>1.01</b>	1.12	1.65	1.31	<b>1.01</b>	<b>−5</b>
	IRI2000	1.34	0.94	<b>1.17</b>	1.29	1.17	1.18	<b>1.17</b>		1.25	1.14	<b>1.07</b>	1.21	1.71	1.27	<b>1.07</b>	
21 Oct. 2001	IRI95	0.86	1.55	<b>2.54</b>	1.76	1.19	1.58	<b>2.54</b>	<b>18</b>	0.83	1.09	<b>3.16</b>	2.10	1.13	1.66	<b>3.16</b>	<b>47</b>
	IRI2000	1.07	1.56	<b>2.10</b>	1.44	1.37	1.51	<b>2.10</b>		0.93	1.33	<b>1.67</b>	1.92	1.32	1.43	<b>1.67</b>	
6 Nov. 2001	IRI95	1.22	<b>2.69</b>	1.54	1.53	1.05	1.60	<b>2.69</b>	<b>5</b>	0.96	<b>3.55</b>	1.83	1.61	1.00	1.79	<b>3.55</b>	<b>23</b>
	IRI2000	1.36	<b>2.54</b>	1.48	1.52	1.05	1.59	<b>2.54</b>		1.08	<b>2.72</b>	1.88	1.60	1.12	1.68	<b>2.72</b>	
24 Nov. 2001	IRI95	1.02	<b>1.72</b>	1.08	1.11	1.32	1.25	<b>1.72</b>	<b>1</b>	1.05	<b>2.59</b>	1.52	1.11	0.99	1.46	<b>2.59</b>	<b>33</b>
	IRI2000	1.06	<b>1.71</b>	1.17	1.01	1.17	1.22	<b>1.71</b>		0.94	<b>1.73</b>	1.15	1.08	1.08	1.20	<b>1.73</b>	

<sup>a</sup>Units are in MHz. Average for the 5-day period and for the storm days are show. Storm days and the related results appear in bold. The percent of improvement (% imp) is calculated for storm days.

the ionospheric storm-time behavior can be captured in an empirical model. STORM, an empirical ionospheric storm-time correction to the  $F$  region ionosphere has been developed over the last few years [Fuller-Rowell *et al.*, 2000, 2001; Araujo-Pradere *et al.*, 2002; Araujo-Pradere and Fuller-Rowell, 2002] and has been incorporated into the IRI2000 [Bilitza, 2001]. The empirical storm model was designed to be a function of the intensity of the storm and depend on latitude and season. STORM was based on an analysis of an extensive database of ionosonde observations, guided by simulations using a coupled thermosphere ionosphere model [Fuller-Rowell *et al.*, 1996].

[4] Araujo-Pradere *et al.* [2003] have recently completed a comprehensive validation of IRI2000 to assess the capabilities in a quantitative statistical way. Table 1 shows the results of the statistical analysis for all the perturbations in the 2000–2001 period. For each of the 14 storms, the RMSE is shown for each day of the 5-day interval for both IRI95 and IRI2000, in the Northern and

Southern Hemisphere separately. The storm days themselves are marked in bold. The results for the Bastille Day will be shown later in detail in Figures 3a and 3b.

[5] The averages columns show the average RMSE for all 5 days and for the storm day or days. The percentage improvement is from comparing the RMSE on the storm days for IRI95 and IRI2000.

[6] Eight of the cases lie within  $\pm 6\%$ , indicating no significant change in the accuracy of the prediction. These cases tend to cluster around the winter hemisphere, a known weak area for the model. All the other 20 cases show significant improvement. Considering all the storms, the STORM model improves the prediction of IRI an average of 34% in the Northern Hemisphere and a 20% in the Southern Hemisphere. Overall the average improvement in performance of IRI2000 is 28%. The results for the particular case of July 2000, presented later in Figure 3, is one of the better cases for the summer hemisphere, with IRI2000 showing a 49% improvement over IRI95.

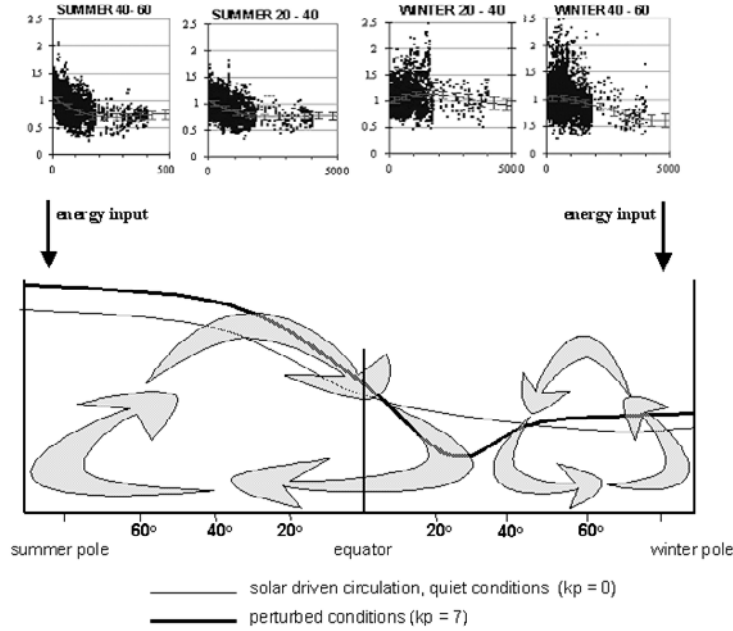


**Figure 1.** Zonally averaged latitudinal structure of the mean molecular mass for quiet (thin shaded line) and perturbed (thick solid line, circulation cells) conditions and its comparison with midlatitude data (top panel).

[7] In this paper we will analyze in detail the response for one of the storms, the well-studied Bastille Day storm in July 2000, and use it to illustrate both the strengths and shortcomings of the model.

## 2. Overview of the Storm Model and Data Sources

[8] Recent investigations have provided some insight and understandings into some of the expected dependencies in the ionospheric response to geomagnetic activity [Rodger *et al.*, 1989; Fuller-Rowell *et al.*, 1996]. The studies indicate that much of the consistent, repeatable characteristics of the storm-time ionosphere response are due to long-lived thermospheric composition changes, which are driven by the integrated effect of Joule heating. On the basis of this knowledge, a model taking into account the prior history of the geomagnetic index  $a_p$  was designed [Fuller-Rowell *et al.*, 2000; Araujo-Pradere *et al.*, 2002]. Such a design includes the seasonal dependence in the migration of the composition bulge by the global wind field, and also includes a nonlinear dependence on the integrated time history of  $a_p$ . The optimum shape of the  $a_p$  index filter (to weight

the time history of the input) was obtained using the singular value decomposition method. The algorithm that describes the empirical model is given by

$$\Phi = \{a_0 + a_1 X(t_0) + a_2 X^2(t_0)\}, \quad (1)$$

where  $\Phi = (f_oF_2 \text{ observed} / f_oF_2 \text{ monthly mean})$ ,  $X(t_0) = \int F(\tau) P(t_0 - \tau) d\tau$ , and  $F(\tau)$  is the filter weighting function of the  $a_p$  index,  $P$ , over the 33 previous hours. The coefficients  $a_0$ ,  $a_1$ , and  $a_2$  have been adjusted to fit the nonlinear relationship between the ionospheric response and the integral of the geomagnetic index  $a_p$ .

[9] The composition theory and observations indicated a seasonal-latitudinal dependence in the ionospheric response to storms. To accommodate this dependence, the model was designed to capture the changing response through the year and over latitude. With this objective, the data has been divided in high (60–80), low (0–20), and two midlatitude bins (20–40, 40–60); and into five seasons, including equinox, summer, and winter solstices, and intermediate seasons.

[10] As an example of the binned database, Figure 1 shows the midlatitudes, solstice conditions data. The top panels show the data for summer and winter conditions in the 20 to 40, and 40 to 60 geomagnetic latitudes. The

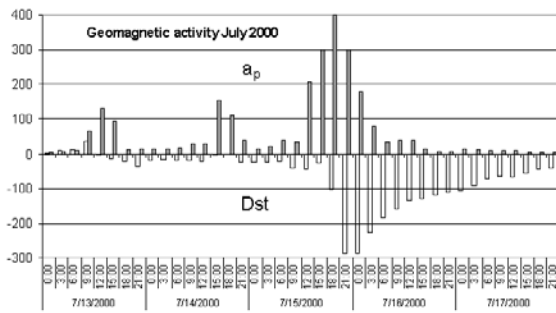


**Figure 2.** Geomagnetic activity for the period of interest.

$y$  axis is the  $f_oF_2$  ratio, and the  $x$  axis is the integral of  $a_p$ . The bottom panel shows the latitudinal structure of the mean molecular mass for quiet and disturbed conditions, together with idealized global circulation cells [cf. Roble, 1986]. Enhancement of the circulation cells can be used to infer changes in neutral composition that can explain the negative phase in the summer hemisphere, and the coexistence of a positive (20–40) and negative (40–60) phases in the winter hemisphere. The so-called “solar circulation” generates, for quiet geomagnetic conditions, a latitudinal profile of the mean molecular mass (thin gray line) that is distorted (thick black line) by the energy input, related to geomagnetic storms, in the auroral regions.

[11] Two points are worthy of note. First, the design of STORM stresses the longer-term integrated effects of geomagnetic activity, and second, that no longitude or local time dependence is considered. We will show that these two points underlie the discrepancies between STORM predictions and the observation for a particular storm.

[12] A real-time version of the model has been implemented, using the hourly values of the 3-hour running  $a_p$ , as provided by the USAF Hourly Magnetometer Analysis Reports. STORM model is now an operational product of the NOAA Space Environment Center. Hourly updates of the model predictions, in the midlatitude and high-latitude bands, can be found at <http://sec.noaa.gov/storm/>.

[13] With a maximum Dst of  $-287.6$  (maximum  $a_p = 400$ ), the storm of July 2000 has been one of the most intense perturbations in the last solar cycle. Figure 2 shows the  $a_p$  and Dst geomagnetic activity indices for this storm period.

[14] Table 2 shows the ionosonde stations included in the July 2000 storm validation study, in each case the station code, the geographic coordinates, and the geomagnetic latitude are given. The stations cover geomagnetic latitudes from  $65.0^\circ\text{N}$  to  $40.6^\circ\text{S}$ , with the best

coverage at midlatitudes in the Northern Hemisphere. The only criterion in the selection of the stations was that data was available in the National Geophysical data Center (NGDC-NOAA) database and that there was reasonable continuity of the ionospheric data ( $f_oF_2$ ) for the period of interest.

[15] For this work,  $f_oF_2$  hourly values for each site were used for a 5-day period of the storm (120 values), in order to see the full picture of the perturbed period. The focus of the quantitative analysis will be on the storm days, when the maximum deviation from the monthly mean occurs.

### 3. Results

[16] Figures 3a and 3b show the response of the ionosphere and the prediction of the models for a 5-day period of the July 2000 storm (13–17 July). For each station, the time evolution of the hourly  $f_oF_2$  is displayed, together with the predictions of both versions of the model, IRI95 without geomagnetic dependence, and IRI2000 with the STORM model included. For this particular storm, the maximum deviation in  $f_oF_2$  from the quiet conditions occurred on the third and fourth days of the 5-day period, the so-called storm days (as defined in the work of Araujo-Pradere et al. [2002]). The information in Figure 3 has been grouped by longitude sector in order to examine the regional dependence in the response for this particular storm, and to highlight both the strengths and weaknesses of the model.

[17] Each figure consists of two regions. Figure 3a includes the European and the Asian sectors, and Figure 3b contains the North American sector, and the South Hemisphere sites. For every plot the black solid line represents the observed  $F$  region critical frequency

**Table 2.** Stations Used in the July 2000 Validation Study

Station	Code	Latitude	Longitude	Geomagnetic Latitude
1 College	CO764	64.9	212.2	65.0
2 Juliusruh/Rugen	JR055	54.6	13.4	54.3
3 Chilton	RL052	51.6	358.7	49.9
4 Wallops Is	WP937	37.8	284.5	49.2
5 Boulder	BC840	40.0	254.7	48.9
6 Novosibirsk	NS355	54.6	83.2	44.2
7 Tortosa	EB040	40.4	0.3	43.6
8 Point Arguello	PA836	34.6	239.4	42.3
9 Eglin AFB	EG931	30.4	273.3	41.1
10 Sofia	SQ143	42.7	23.4	41.0
11 San Vito	VT139	40.6	17.8	34.4
12 Anyang	AN438	37.4	127.0	29.5
13 Learmonth	LM42B	$-21.9$	114.0	$-33.0$
14 Grahamstown	GR13L	$-33.3$	26.5	$-33.9$
15 Port Stanley	PSJ5J	$-51.7$	302.2	$-40.6$

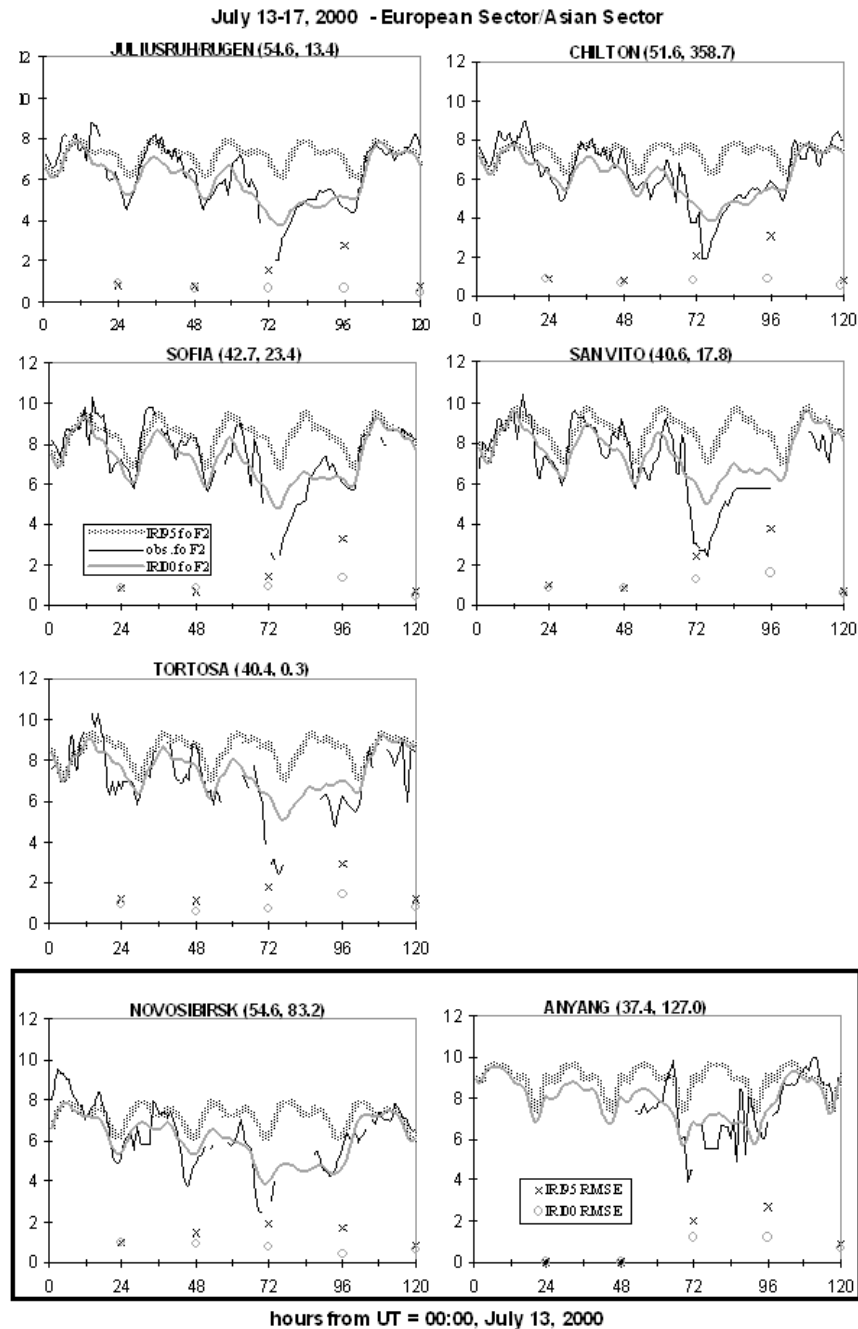


**Figure 3a.** Data and output of the IRI95 and IRI2000 models at five locations in the European sector, and two locations (framed plots) in the Asian sector for the Bastille Day storm. The dotted line shows IRI95, the solid black line is the observation, and the gray line show IRI2000. Note that for Southern Hemisphere stations (winter), the output of IRI95 and IRI2000 are almost coincident, so the dotted line is sometimes hidden behind the gray line.



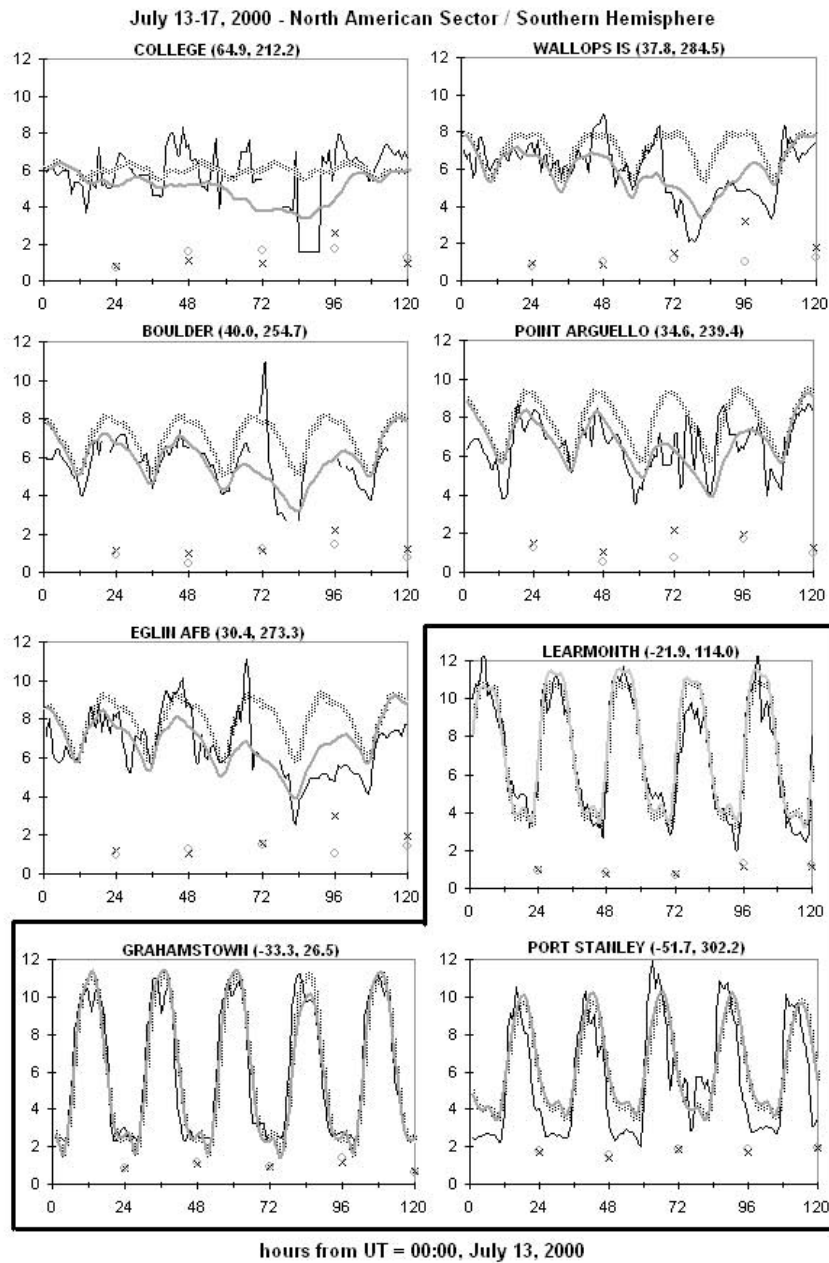


**Figure 3b.** Same as Figure 3a but for five locations in the North American sector and three locations (framed plots) in the Southern Hemisphere.

( $f_oF_2$ ), while the dotted line is the IRI95 output and the thick gray line corresponds to the IRI2000 output. A symbol in matching color (black cross for IRI95, gray circle for IRI2000) represents the daily root mean square

error ( $RMSE = ((\sum(model - data)^2)/24)^{0.5}$ ) for each set of data, as calculated for the previous 24 hours.

[18] The  $x$  axis corresponds to time, from 0000 UT of the first day of the period (13 July) up to the 120th hour.

The  $y$  axis is the ratio of  $f_oF_2$  for both the data and the model output. This axis also quantifies the RMSE, the metric used to assess the quality of the predictions.

[19] The first observation from Figures 3a and 3b is the ability of the model to capture the general direction of the changes. For the nonstorm days (first, second, and fifth days for this particular storm), there are no significant difference between the prediction and the monthly mean RMSE. For the third and fourth day in the northern summer stations, there is a clear tendency for a negative phase, and the model captures its direction and magnitude reasonably well. This is not the case for the southern hemisphere winter stations, where the data is less consistent. The lack of a clear direction to the response in winter makes model predictions challenging, but at least the empirical model does not overpredict the response.

[20] A detailed analysis of Figure 3 shows some consistent characteristics of the STORM prediction in both its strengths and shortcomings. In the top panels of Figure 3a, corresponding to the European sector, it can be observed that the STORM model consistently followed the trend of the data, but it missed the full depth of the depression in  $f_oF_2$  at hour 72, a common ionospheric feature of all the European sites.

[21] Clearly, STORM is not capturing the full development of the negative phase of the storm, missing up to 40% of the depth of the depression at hour 72 in most of the European sites. Part of this is probably due to the extreme nature of the Bastille Day storm, the largest of the present solar cycle, and somewhat on the edge of the statistical distribution of storms magnitude used to develop the model. We expect part is also due to the regional nature of the composition changes that are causing the deep depressions. Localized auroral heating will cause structure in the composition changes that are difficult to capture in an empirical model. Most likely the deep ionospheric depression seen over Europe is a consequence of these localized composition changes.

[22] One of the Asian sector sites, Novosibirsk, in the lower of the panels of Figure 3a, has a similar response to the European sector, with a big depression at hour 72 exceeding the prediction of the model. The other Asian station, Anyang, presents a behavior more resembling the North American sector (discussed next), with a positive phase early in the storm, which is not captured by the model. At both Asian sites, the STORM model matches fairly well the general trend of the storm response.

[23] The top panel of Figure 3b corresponds to five sites in the North American sector. Apart from College and Point Arguello, where the poor data makes the analysis difficult, the rest of the sites show a positive phase storm commencement that STORM does not capture, although it closely follows the subsequent negative phase. In the particular case of Wallops Island,

the model recovers too soon, missing the depression at hour 96.

[24] In the North American sector, in general, STORM model followed very well the trend of the ionospheric response but misses the sharp positive phase, and then slightly underpredicted the following negative phase. The input of the model (integral of  $a_p$  over the previous 33 hours) makes it difficult to capture high-frequency features. A way to answer this problem may be to design an additional, short-period filter, obtained from the residuals (model output - observed values) of the storm sample. Currently, however, no sharp response is modeled by STORM.

[25] Figure 3b bottom panel, winter at Southern Hemisphere, is a well-known weak area of the model. IRI2000, and IRI95, failed to predict the local ionosphere departure from quiet conditions behavior. Extensive work is required in order to improve the STORM winter predictions.

[26] Summarizing, STORM model followed the general trend of the ionospheric response for the July 2000 event, but it failed to capture the depth of some features, or the rapid rises and sharp responses, even some that cover whole regions (i.e., depth of negative phase at the European sector, positive phase at the North American sector).

## 4. Conclusion

[27] The detailed comparison of STORM with data from the Bastille Day event illustrates both the strengths and shortcomings of the model. From the previous quantitative validation study, it is clear that the new storm model is an improvement on the previous IRI95 version, which had no geomagnetic activity dependence. In fact, the RMSE statistics for the Bastille Day storm shows that the model performed particularly well for this period. Table 1 showed that the RMSE error on the storm days showed almost a 50% improvement. The extreme nature of the event, however, also illustrates the areas where improvement is still needed in the empirical description.

[28] There are two main areas that could be targeted in the future: the initial rapid positive ionospheric response at the onset of the disturbance, and the regional nature of the negative phase where one longitude sector is harder hit than another. Note that the algorithms used in the model have no local time or longitude dependence, so a different scaling of the magnitude of the response to fit one sector would simply worsen the fit in another. In both cases, additional information is required.

[29] The longitude dependence of the negative phase most likely reflects the regional nature of the composition disturbances. To address this aspect requires revisiting the possibility of a local time dependence in the response. This can either arise from the UT time history of an event, where the local time position of particular longitude sector

during the main energy injection from the magnetosphere will vary from storm to storm. On the other hand, the local time dependence can arise from transport of the diurnal or storm induced wind fields. Note that *Rodger et al.* [1989] were able to pick up significant local time dependence in the ionospheric response to storms.

[30] The second aspect, that of the rapid onset of the positive phase, will require another solution. The nature of the current algorithm requires integrating the time history of the 3-hour  $a_p$  geomagnetic index over the previous 33 hours. This tends to suppress the possibility of a rapid response. This could be addressed in the future by including an additional dependence on the  $a_p$  index itself, rather than an integral over time.

## References

- Araujo-Pradere, E. A., and T. J. Fuller-Rowell (2000), A model of a perturbed ionosphere using the auroral power as the input, *Geof. Int.*, *39*(1), 29–36.
- Araujo-Pradere, E. A., and T. J. Fuller-Rowell (2002), STORM: An empirical storm-time ionospheric correction model, 2, Validation, *Radio Sci.*, *37*(5), 1071, doi:10.1029/2002RS002620.
- Araujo-Pradere, E. A., T. J. Fuller-Rowell, and M. V. Codrescu (2002), STORM: An empirical storm-time ionospheric correction model, 1, Model description, *Radio Sci.*, *37*(5), 1070, doi:10.1029/2001RS002467.
- Araujo-Pradere, E. A., T. J. Fuller-Rowell, and D. Bilitza (2003), Validation of the STORM response in IRI2000, *J. Geophys. Res.*, *108*(A3), 1120, doi:10.1029/2002JA009720.
- Bilitza, D. (2001), International Reference Ionosphere 2000, *Radio Sci.*, *36*(2), 261–275.
- Bilitza, D., K. Rawer, L. Bossy, and T. Gulyaeva (1993), International Reference Ionosphere—Past, present, future, *Adv. Space Res.*, *13*(3), 3–23.
- Fuller-Rowell, T. J., M. V. Codrescu, H. Rishbeth, R. J. Moffet, and S. Quegan (1996), On the seasonal response of the thermosphere and ionosphere to geomagnetic storms, *J. Geophys. Res.*, *101*(A2), 2343–2353.
- Fuller-Rowell, T. J., E. A. Araujo-Pradere, and M. V. Codrescu (2000), An empirical ionospheric storm-time correction model, *Adv. Space Res.*, *25*(1), 139–148.
- Fuller-Rowell, T. J., M. V. Codrescu, and E. A. Araujo-Pradere (2001), Capturing the storm-time ionospheric response in an empirical model, in *Space Weather, AGU Geophys. Monogr. Ser.*, vol. 125, pp. 393–401, edited by P. Song, H. Singer, and G. Siscoe, AGU, Washington, D. C.
- Roble, R. G. (1986), Chemistry in the thermosphere and ionosphere, *Chem. Eng. News*, *64*(24), 23–28.
- Rodger, A. S., G. L. Wrenn, and H. Rishbeth (1989), Geomagnetic storms in the Antarctic F region, II, physical interpretation, *J. Atmos. Terr. Phys.*, *51*, 851–866.

---

E. A. Araujo-Pradere and T. J. Fuller-Rowell, SEC-NOAA, 325 Broadway R/SEC, Boulder, CO 80305, USA. (eduardo.araujo@noaa.gov)

D. Bilitza, Raytheon ITSS/Goddard Space Flight Center, Code 632, Greenbelt, MD 20771, USA.